

# Twisted-light-induced intersubband transitions in quantum wells at normal incidence

B. Sbierski

<sup>1</sup>*Physik-Department, Technische Universität München,  
James-Frank-Str. 1, 85748 Garching, Germany*

G. F. Quinteiro and P. I. Tamborenea

<sup>2</sup>*Departamento de Física and IFIBA, FCEN,  
Universidad de Buenos Aires, Ciudad Universitaria,  
Pab. I, Ciudad de Buenos Aires, Argentina*

We examine theoretically the intersubband transitions induced by laser beams of light with orbital angular momentum (twisted light) in semiconductor quantum wells at normal incidence. These transitions become possible in the absence of gratings thanks to the fact that collimated laser beams present a component of the light's electric field in the propagation direction. We derive the matrix elements of the light-matter interaction for a Bessel-type twisted-light beam represented by its vector potential in the paraxial approximation. Then, we consider the dynamics of photo-excited electrons making intersubband transitions between the first and second subbands of a standard semiconductor quantum well. Finally, we analyze the light-matter matrix elements in order to evaluate which transitions are more favorable for given orbital angular momentum of the light beam in the case of small semiconductor structures.

PACS numbers: 78.20.Bh, 78.20.Ls, 78.40.Fy, 42.50.Tx

Keywords:

## INTRODUCTION

Quantum wells are a fundamental and well-studied type of man-made semiconductor nanostructure [1]. They can exhibit remarkable transport phenomena and their optical properties have motivated intense basic research and numerous applications. In particular, intersubband transitions, that is, light-induced transitions between states of a given energy band belonging to different subbands, have been extensively studied and successfully applied to the development of infrared lasers and detectors [2]. In parallel to these developments in the area of semiconductor nanoscience and technology, a new branch of optics developed vigorously in the last twenty years, namely, the study of phase-structured light [3]. The generation and applications of *twisted light* (TL), or

light beams carrying *orbital* angular momentum, gained great attention after the seminal work of Allen *et al.* [4] The interaction of TL with mesoscopic particles (optical tweezers) [5–7], atoms and molecules [8, 9], and Bose-Einstein condensates [10, 11] has been studied recently. Other issues, like the theoretical description of cavity-QED of TL [12] and the use of TL for potential applications in quantum information processing [13] have also been addressed [14].

The interaction of TL with solid-state systems thus appears as a promising field of research and technology. A number of basic situations have recently been investigated theoretically [15–22], but fewer experimental studies have been reported thus far [23, 24]. In this article we initiate the study of intersubband transitions induced by TL beams in semiconductor quantum wells. Besides considering the intersubband excitation with TL, we focus on a special geometry that has not received much attention thus far: By taking advantage of the fact that collimated laser beams possess a component of the electric field along the propagation direction, we propose the excitation of intersubband transitions at normal incidence without using gratings. Thus, collimated beams of TL bring about two nonstandard ingredients to intersubband transitions: new selection rules based on the conservation of the spin and *orbital* angular momentum, and the possibility of excitation at normal incidence.

## TWISTED LIGHT

Let us consider a TL beam with a radial dependence of the Bessel type and circular polarization  $\sigma = \pm 1$ . In the Coulomb gauge ( $\nabla \cdot \mathbf{A} = 0$ ) its vector potential in the paraxial approximation is given by [25, 26]

$$\mathbf{A}(\mathbf{r}, t) = A_0 e^{i(q_z z - \omega t)} \left[ \boldsymbol{\epsilon}_\sigma J_\ell(q_r r) e^{i\ell\phi} - i\sigma \mathbf{e}_z \frac{q_r}{q_z} J_{\ell+\sigma}(q_r r) e^{i(\ell+\sigma)\phi} \right] + c.c., \quad (1)$$

with  $\boldsymbol{\epsilon}_\sigma = \mathbf{e}_x + i\sigma\mathbf{e}_y$ , Bessel functions  $J_\ell$ , and  $q_r^2 + q_z^2 = \omega^2/c^2$ . The light's orbital angular momentum is given by the integer  $\ell$ . When optical transitions can be excited by both the  $xy$  and the  $z$  components of the light's electric field, the  $z$ -component of the vector potential is normally neglected since usually  $q_r \ll q_z$ . On the other hand, there are experimental situations where the component of the field in the plane of the absorbing material ( $xy$ -plane) cannot induce quantum transitions due to symmetry restrictions while the  $z$ -component can. This is the case of intersubband transitions in quantum-well and quantum-disk structures at normal incidence, which is the situation we focus on here. Moreover, advances in optical hyperlenses suggest that highly collimated beams (with large  $q_r$ ) can be obtained [27]. Optical transitions induced by the  $xy$ -component of the TL beam

in bulk [15, 18], quantum wells [18], and quantum dots [16] have been studied recently.

### SEMICONDUCTOR QUANTUM WELL

In order to model the semiconductor quantum well in a convenient and flexible way we consider a cylindrical disk of height  $z_0$  and radius  $r_0$ . The limit of  $r_0 \rightarrow \infty$  describes the infinite quasi-two-dimensional quantum well system, and the finite  $r_0$  case will allow us to do numerical modeling with realistic beam and nanostructure parameters. Note that the chosen cylindrical geometry is convenient from a mathematical and conceptual point of view, given the cylindrical nature of the beam [18]. We have in mind standard quantum wells made of, for example, GaAlAs [1]. With hard-wall confinement, the envelope-function eigenstates of the cylindrical disk are given by

$$\psi_{nm\nu}(r) = \mathcal{N}_{m\nu} J_m(q_{m\nu} r) e^{im\phi} \sqrt{\frac{2}{\pi z_0}} \sin\left(\frac{n\pi z}{z_0}\right), \quad (2)$$

with  $q_{m\nu} = x_{m\nu}/r_0$ ,  $x_{m\nu}$  being the  $\nu$ -th zero of the Bessel function  $J_m$ ,  $n = 1, 2, \dots$  the subband index, and the normalization constant

$$\mathcal{N}_{m\nu} = \frac{1}{r_0 J'_m(x_{m\nu})}. \quad (3)$$

The eigen-energies are

$$\varepsilon_{nm\nu} = \frac{\hbar^2}{2m_e^*} \left( q_{m\nu}^2 + \frac{\pi^2 n^2}{z_0^2} \right), \quad (4)$$

where  $m_e^*$  is the effective electron mass in the band under consideration.

### LIGHT-MATTER INTERACTION MATRIX ELEMENTS

The intersubband transitions are governed by the matrix elements of the electron-TL interaction,  $h_I$ , whose matrix elements

$$\langle n'm'\nu' | h_I | nm\nu \rangle = -\frac{e}{m_e} \langle n'm'\nu' | \mathbf{A} \cdot \mathbf{p} | nm\nu \rangle + \frac{e^2}{2m_e^*} \langle n'm'\nu' | \mathbf{A}^2 | nm\nu \rangle \quad (5)$$

need to be worked out ( $e = -|e|$  and  $m_e$  are the electron charge and bare mass, respectively). It can be easily shown that, under normal incidence, the  $A_x$  and  $A_y$  components of the vector potential do not contribute to the matrix elements for intersubband processes ( $n' \neq n$ ). Intraband transitions are strongly suppressed by the smallness of their light-matter matrix elements (between “in-plane” single-particle states). Also, considering typical intersubband frequencies of  $\hbar\omega \simeq 100$  meV, both intraband single-particle excitations and surface plasmons are completely off-resonance. Thus,

intrasubband effects can be safely ignored here. For the component  $A_z$  we obtain from the linear term of the interaction

$$-\frac{e}{m_e} \langle n' m' \nu' | A_z p_z | n m \nu \rangle = \frac{2\pi\sigma e \hbar A_0 q_r}{m_e q_z} \eta_{m' \nu', m \nu} B_{n' n} (\delta_{m' - m, \ell + \sigma} e^{-i\omega t} - \delta_{m' - m, -(\ell + \sigma)} e^{i\omega t}), \quad (6)$$

where

$$B_{n' n} = \frac{2nn'}{n'^2 - n^2} \delta_{n' + n, \text{odd}}, \quad (7)$$

$$\eta_{m' \nu', m \nu} = \mathcal{N}_{m' \nu'} \mathcal{N}_{m \nu} \int_0^{r_0} r dr J_{m'}(q_{m' \nu'} r) J_{\ell + \sigma}(q_r r) J_m(q_{m \nu} r). \quad (8)$$

The factor  $B_{n' n}$  has been obtained under the dipole moment approximation (applied only in the  $z$ -direction),  $q_z z_0 \ll 1$ , which is amply justified in our system. For transitions between subbands 1 and 2, we have  $B_{21} = \frac{4}{3} = -B_{12}$ . Within the same dipole approximation, the quadratic term is proportional to  $\delta_{n' n}$  and therefore drops out for intersubband transitions. The Kronecker deltas that appear in Eq. (6) enforce the conservation of angular momentum. Since the electron undergoes an intraband transition, there is obviously no change in the angular momentum associated with the periodic part of its Bloch wave function. As a consequence, the spin angular momentum of the photon ( $\sigma$ ), which in interband transitions accounts for the change in the band angular momentum of the electron [15], appears now in the selection rules for the envelope function along with the photon's orbital angular momentum ( $\ell$ ), as seen also in the study of intraband transitions in quantum rings [17, 28].

The matrix elements of Eq. (6) involve integrals with three Bessel functions [see Eq. (8)] which, to the best of our knowledge, do not admit an analytical solution and are somewhat numerically demanding. However, they can be simplified in cases of practical interest where the semiconductor structure is small compared to the beam waist. This wide-beam approximation has the advantage of keeping the interesting angular dependence of TL while simplifying the radial dependence which is not essential for our purposes. Let us consider a typical quantum well with intersubband transition energy of  $\hbar\omega \simeq 100$  meV. Now,  $q_r^2 + q_z^2 = \omega^2/c^2$  with  $q_r \ll q_z$  implies that  $q_r \ll \omega/c = 8.3 \times 10^5 \text{ m}^{-1}$ , and therefore the first zero of the beam's Bessel function is at least a few hundred microns from the center of the beam. Then, for a large quantum disk of a few tens of microns centered at the beam axis we can approximate the beam's Bessel function by the first term of its series expansion. Furthermore, according to Eq. (6), only the values of  $m' = m \pm (\ell + \sigma)$  (+ for absorption and - for

emission) lead to non-vanishing matrix elements. Then

$$\begin{aligned} \eta_{m\pm(\ell+\sigma),\nu';m\nu} &= \mathcal{N}_{m\pm(\ell+\sigma),\nu'} \mathcal{N}_{m,\nu} \int_0^{r_0} r dr J_{m\pm(\ell+\sigma)}(q_{m\pm(\ell+\sigma),\nu'} r) J_{\ell+\sigma}(q_r r) J_m(q_{m\nu} r) \\ &\simeq \frac{\mathcal{N}_{m\pm(\ell+\sigma),\nu'} \mathcal{N}_{m,\nu} r_0^2}{\Gamma(\ell+2)} \left(\frac{q_r r_0}{2}\right)^{\ell+\sigma} \int_0^1 du J_{m\pm(\ell+\sigma)}(x_{m\pm(\ell+\sigma),\nu'} u) J_m(x_{m\nu} u) u^{\ell+\sigma+1}. \end{aligned} \quad (9)$$

## PHYSICAL INTERPRETATION

The matrix elements obtained in the previous section permit the calculation of the different forms of optical response of the quantum well to normally incident twisted light. Equations of motion for the single-particle density matrix provide a general theoretical framework for such calculations, and can be straightforwardly obtained, in the free-carrier regime, for example from Ref. [18]. Here, we will examine some basic aspects of the dynamics of the photoexcited electrons and argue for the detectability of the proposed intersubband transitions.

A central quantity to describe the dynamics of the photoexcited electrons is the population  $\rho_{2m\nu}(t)$  of the second subband states with quantum numbers  $(m, \nu)$ . In the perturbative regime these populations can be obtained through the equations of motion that we just mentioned [18], or more directly via ordinary time-dependent perturbation theory [29]. To second order in the light field and assuming a laser pulse turned on at  $t = 0$  one obtains for the population of the second-subband states

$$\begin{aligned} \rho_{2m\nu}^{(2)}(t) &= 4 \left( \frac{2\pi e \hbar A_0 q_r}{m_e q_z} \right)^2 \sum_{\nu'} f_{m-\ell-\sigma,\nu'} \eta_{m\nu;m-\ell-\sigma,\nu'}^2 B_{21}^2 \\ &\times \frac{\sin^2[(\varepsilon_{2m\nu} - \varepsilon_{1,m-\ell-\sigma,\nu'} - \hbar\omega)t/2\hbar]}{(\varepsilon_{2m\nu} - \varepsilon_{1,m-\ell-\sigma,\nu'} - \hbar\omega)^2}, \end{aligned} \quad (10)$$

where  $f_{m-\ell-\sigma,\nu'}$  is the Fermi distribution that gives the initial populations of the first-subband states. From this expression one obtains the Fermi-Golden-Rule linear time dependence in the long-time limit, and for short pulses the time-dependence is quadratic.

In order to get some insight into the optical excitation and the resulting population of the second subband in the situation of small nanostructures, we have performed numerical calculations of  $\eta$  in the case of  $m' = m + \ell + \sigma$ . From Eq. (10), one would like to understand what contributes to the population of a particular state  $(m, \nu)$  of the second subband. In Fig. 1 we plot  $\eta^2$  (we plot  $\eta^2$  rather than  $\eta$  since it has the visual advantage of not presenting oscillations from positive to negative values), as a function of  $\nu'$  for fixed values of  $\nu = 30$  and  $\ell = 10$ , and two different values of  $m$ . One immediately recognizes that there are several states  $\nu'$  of the first subband contributing

to the second subband population. This is the main difference with the case of vertical (one-to-one) transitions induced by plane-waves, and has been already discussed in a previous paper [15]. Furthermore, we observe a strong shift in the peak position, moving to higher values of  $\nu'$  for larger values of  $m$ .

In Fig. 2 we plot  $\eta^2$  for a fixed value of  $\nu = 30$  and three different values of  $\ell$  and  $m$ . This figure shows that for small  $\ell$  few states  $\nu'$  away from  $\nu$  are significantly excited, resembling vertical transitions. Thus, for small values of  $\ell$ , it might be reasonable to simplify expression (10) by eliminating the sum and evaluating only the term with  $\nu' = \nu$ . However, for increasing values of  $\ell$ , more states with different  $\nu'$  contribute and the whole sum in Eq. (10) should be kept. From this figure we see that there is also an  $\ell$ -dependent shift of the peak away from the value  $\nu' = \nu$ , which in our figure was chosen so as to cancel the  $m$ -induced shift.

Intersubband transitions are traditionally detected using relative absorbance measurements in multi-quantum-well structures [30]. Normally, the transitions are produced by the transverse component of the light's electric field at oblique incidence. It is thus worth comparing the relative strength of those transitions to our proposed normal-incidence transitions. A simple estimate can be done by comparing the ratio of the longitudinal to the perpendicular component of the vector potential given in Eq. (1). This ratio is given roughly by  $q_r/q_z$ , which can be chosen in the laboratory fairly freely. If  $q_r/q_z \approx 0.1$ , then the population of the second subband states is roughly a hundred times smaller than in the usual scheme. Given the available laser powers this reduction does not represent a significant experimental limitation. Alternatively, a pump-and-probe experimental scheme would also be adequate to observe the normal-incidence photoexcitation examined here.

## CONCLUSION

We have briefly analyzed the viability of inducing intersubband transitions in semiconductor quantum wells at normal incidence with twisted light beams. These transitions are enabled by the component of the electric field in the propagation direction which is present in collimated beams. We obtained the matrix elements of the light-matter interaction, which display the conservation law associated to the transfer of both spin and orbital angular momentum from the light to the electrons in doped quantum wells. A simplified expression for the matrix elements, valid in the standard case of a somewhat small semiconductor system—as compared to the laser beam waist—was presented and computed numerically. Using the population of the second subband to second

order in the field, we argued for the feasibility of the intersubband transitions induced by twisted light at normal incidence.

### Acknowledgments

We acknowledge financial support from the Cooperation Program ANPCyT–Max-Planck Society, through grant PICT-2006-02134, and from the University of Buenos Aires, through grants UBACYT 2008/2010–X495 and 2011/2014–20020100100741.

- 
- [1] John H. Davies, *The Physics of Low-dimensional Semiconductors: An Introduction* (Cambridge University Press, 1997).
  - [2] Roberto Paiella, *Intersubband Transitions in Quantum Structures* (The McGraw-Hill Companies, 2006).
  - [3] David L. Andrews, *Structured Light and Its Applications: An Introduction to Phase-Structured Beams and Nanoscale Optical Forces* (Academic Press, 2008).
  - [4] L. Allen, M. W. Beijersbergen, R. J. C. Spreeuw, and J. P. Woerdman, Phys. Rev. A **45**, 8185 (1992).
  - [5] S. Barreiro and J. W. R. Tabosa, Phys. Rev. Lett. **90**, 133001 (2003).
  - [6] B. Allen, J. Opt. B. Quantum Semiclass. Opt. **4**, S1-S6 (2002).
  - [7] M. E. J. Friese, T. A. Nieminen, N. R. Heckenberg, and H. Rubinsztein-Dunlop, Nature **394**, 348 (1998).
  - [8] B. L. C. Dávila-Romero, D. L. Andrews, and M. Babiker, J. Opt. B. Quantum Semiclass. Opt. **4**, S66-S72 (2002).
  - [9] F. Araoka, T. Verbiest, K. Clays, and A. Persoons, Phys. Rev. A **71**, 055401 (2005).
  - [10] M. F. Andersen, C. Ryu, P. Clade, V. Natarajan, A. Vaziri, K. Helmerson, and W. D. Phillips, Phys. Rev. Lett. **97**, 170406 (2006).
  - [11] T. P. Simula, N. Nygaard, S. X. Hu, L. A. Collins, B. I. Schneider, and K. Molmer, Phys. Rev. A **77**, 015401 (2008).
  - [12] S. Al-Awfi and M. Babiker, Phys. Rev. A **61**, 033401 (2000).
  - [13] B. A. Muthukrishnan and C. R. Stroud Jr., J. Opt. B. Quantum Semiclass. Opt. **4**, S73-S77 (2002).
  - [14] L. Allen, S. M. Barnett, and M. J. Padgett, *Optical Angular Momentum* (Institute of Physics, 2003).
  - [15] G. F. Quinteiro and P. I. Tamborenea, EPL **85**, 47001 (2009).
  - [16] G. F. Quinteiro and P. I. Tamborenea, Phys. Rev. B **79**, 155450 (2009).
  - [17] G. F. Quinteiro and J. Berakdar, Opt. Express **17**, 20465 (2009).
  - [18] G. F. Quinteiro and P. I. Tamborenea, Phys. Rev. B **82**, 125207 (2010).

- [19] G. F. Quinteiro, A. O. Lucero, and P. I. Tamborenea, J. Phys.: Condens. Matter **22**, 505802 (2010).
- [20] G. F. Quinteiro, EPL **91**, 27002 (2010).
- [21] J. Wätzel, A. S. Moskalenko, and J. Berakdar, Opt. Express **20**, 27792 (2012).
- [22] K. Köksal and J. Berakdar, Phys. Rev. A **86**, 063812 (2012).
- [23] Y. Ueno, Y. Toda, S. Adachi, R. Morita, and T. Tawara, Opt. Express **22**, 20567 (2009).
- [24] N. B. Clayburn, J. L. McCarter, J. M. Dreiling, M. Poelker, D. M. Ryan, and T. J. Gay, Phys. Rev. B **87**, 035204 (2013).
- [25] K. Volke-Sepulveda, V. Garcés-Chávez, S. Chávez-Cerda, J. Arlt, and K. Dholakia, J. Opt. B: Quantum Semiclass. Opt. **4**, S82 (2002).
- [26] R. Jáuregui, Phys. Rev. A **70**, 033415 (2004).
- [27] Jiangnan Zhao, Guixing Zheng, Song Li, Hui Zhou, Yue Ma, Ruiying Zhan, Yan Shi, and Ping'an He. Chinese Optics Lett. **10**, 042302 (2012).
- [28] G. F. Quinteiro, P. I. Tamborenea, and J. Berakdar, Opt. Express **19**, 26733-26741 (2011).
- [29] L. D. Landau and E. M. Lifshitz, *Quantum Mechanics, Non-Relativistic Theory* (Pergamon Press, 1977), section 42.
- [30] L. C. West and S. J. Eglash, Appl. Phys. Lett. **46**, 1156 (1985).

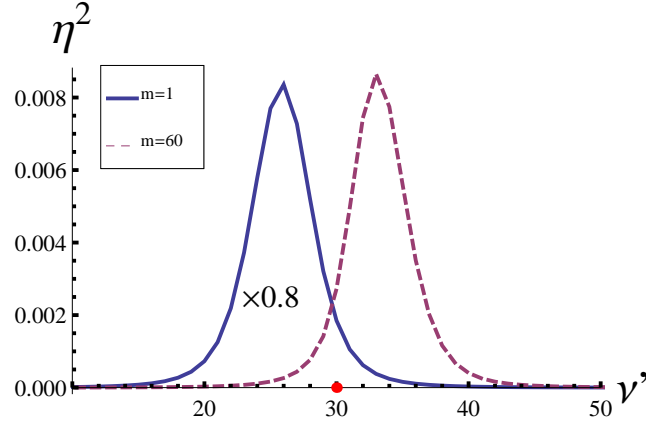


FIG. 1: Integral  $\eta$  squared as a function of  $\nu'$  with  $m' = m + \ell + \sigma$  and for fixed values of  $\nu = 30$ ,  $\ell = 10$ , and  $\sigma = 1$ , and two different values of  $m$ . Notice the  $m$ -dependent shift in the peak position.



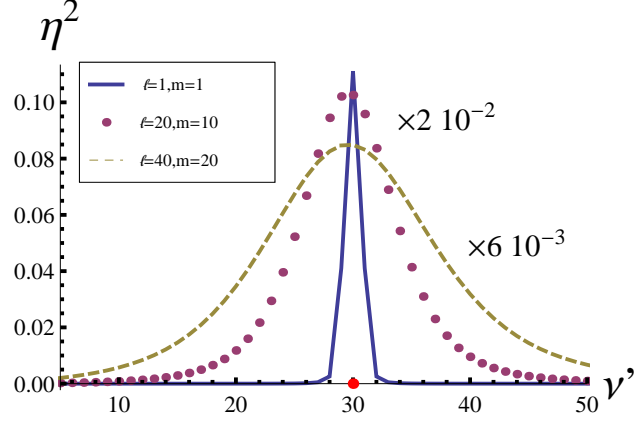


FIG. 2: Integral  $\eta$  squared as a function of  $\nu'$  with  $m' = m + \ell + \sigma$  for a fixed value of  $\nu = 30$  and  $\sigma = 1$ , and three different values of  $\ell$  and  $m$ . The OAM  $\ell$  affects many features: i) the width, ii) the amplitude and iii) the shift of the peak position. The shift of the peak also depends on the value of  $m$ , but that change is opposite to that of  $\ell$ : the plot shows how the shifts produced by  $m$  and  $\ell$  can compensate each other and produce responses roughly centered at  $\nu = \nu'$ .